$$\times \Gamma\left(i+\frac{m_k}{2}+\frac{3}{2}\right)\left(-4\tau\Omega_k^2 p_u^2 N\right)^i x^{-2v(i+1)+1}\,dx$$
$$= \frac{\tau\Omega_k^2 p_u^2 N 2^{m_k}\Gamma\left(\frac{v-1}{v}\right)\Gamma\left(\frac{m_k}{2}+\frac{1}{2}\right)\Gamma\left(\frac{m_k}{2}+1\right)}{\left(R^2-R_0^2\right)v\sqrt{\pi}\ln(2)\Gamma(m_k)\Gamma\left(\frac{v-1}{v}+1\right)}$$
$$\times \sum_{i=0}^{\infty}\frac{\Gamma(i+1)\Gamma(2)\Gamma\left(i+\frac{v-1}{v}\right)\Gamma\left(\frac{v-1}{v}+1\right)}{\Gamma(1)\Gamma(i+2)\Gamma\left(\frac{v-1}{v}\right)\Gamma\left(i+\frac{v-1}{v}+1\right)}$$
$$\times \frac{\Gamma\left(i+\frac{m_k}{2}+\frac{1}{2}\right)\Gamma\left(i+\frac{m_k}{2}+1\right)\Gamma(i+1)}{\Gamma\left(\frac{m_k}{2}+\frac{1}{2}\right)\Gamma\left(\frac{m_k}{2}+1\right)\Gamma(1)}$$
$$\times \left(\frac{1}{R_0^{2v-2}}\frac{\left(\frac{-4\tau\Omega_k^2 p_u^2 N}{R_0^{2v}}\right)^i}{\Gamma(i+1)}-\frac{1}{R^{2v-2}}\frac{\left(\frac{-4\tau\Omega_k^2 p_u^2 N}{R^{2v}}\right)^i}{\Gamma(i+1)}\right). \quad (35)$$

Based on the definition of Pochmann symbol and together with [19, eq. (16.2.1)], the derivation of $\int_{R_0}^{R} x\Xi_1(x, m_k, p_u, v)\,dx$ is completed. The derivation of $\int_{R_0}^{R} x\Xi_2(x, m_k, p_u, v)\,dx$ is similar to Appendix B, where N in Appendix B is replaced with τ. Thus, we end the whole proof.

ACKNOWLEDGMENT

The authors would like to thank the anonymous reviewers for their valuable and professional comments, which have greatly improved the quality of this paper.

REFERENCES

[1] Y. Jing and B. Hassibi, "Distributed space–time coding in wireless relay networks," *IEEE Trans. Wireless Commun.*, vol. 5, no. 12, pp. 3524–3536, Dec. 2006.
[2] S. Jin, M. R. McKay, C. Zhong, and K.-K. Wong, "Ergodic capacity analysis of amplify-and-forward MIMO dual-hop systems," *IEEE Trans. Inform. Theory*, vol. 56, no. 5, pp. 2204–2224, May 2010.
[3] T. L. Marzetta, "Noncooperative cellular wireless with unlimited numbers of base station antennas," *IEEE Trans. Wireless Commun.*, vol. 9, no. 11, pp. 3590–3600, Nov. 2010.
[4] H. Q. Ngo, E. G. Larsson, and T. L. Marzetta, "Energy and spectral efficiency of very large multiuser MIMO systems," *IEEE Trans. Commun.*, vol. 61, no. 4, pp. 1436–1449, Apr. 2013.
[5] J. Zhang, C.-K. Wen, S. Jin, X. Gao, and K.-K. Wong, "On capacity of large-scale MIMO multiple access channels with distributed sets of correlated antennas," *IEEE J. Sel. Areas Commun.*, vol. 31, no. 2, pp. 133–148, Feb. 2013.
[6] H. Cramér, *Random Variables and Probability Distributions*. Cambridge, U.K.: Cambridge Univ. Press, 1970.
[7] A. Laourine, M.-S. Alouini, S. Affes, and A. Stéphenne, "On the capacity of generalized-K fading channels," *IEEE Trans. Wireless Commun.*, vol. 7, no. 7, pp. 2441–2445, Jul. 2008.
[8] P. M. Shankar, "Error rates in generalized shadowed fading channels," *Wireless Pers. Commun.*, vol. 28, no. 3, pp. 233–238, Feb. 2004.
[9] P. S. Bithas, N. C. Sagias, P. T. Mathiopoulos, G. K. Karagiannidis, and A. A. Rontogiannis, "On the performance analysis of digital communications over generalized-K fading channels," *IEEE Commun. Lett.*, vol. 10, pp. 353–355, May 2006.
[10] I. M. Kostić, "Analytical approach to performance analysis for channel subject to shadowing and fading," *Proc. Inst. Electr. Eng.—Commun.*, vol. 152, no. 6, pp. 821–827, Dec. 2005.
[11] P. S. Bithas, P. T. Mathiopoulos, and S. A. Kotsopoulos, "Diversity reception over generalized-K (K_G) fading channels," *IEEE Trans. Wireless Commun.*, vol. 6, no. 12, pp. 4238–4243, Dec. 2007.
[12] L. Wu, J. Lin, K. Niu, and Z. He, "Performance of dual-hop transmissions with fixed gain relays over generalized-K fading channels," in *Proc. IEEE Int. Conf. Commun.*, Jun. 2009, pp. 1–5.
[13] C. Zhong, K.-K. Wong, and S. Jin, "Capacity bounds for MIMO Nakagami-m fading channels," *IEEE Trans. Signal Process.*, vol. 57, no. 9, pp. 3613–3623, Sep. 2009.
[14] M. K. Simon and M.-S. Alouini, *Digital Communication over Fading Channels—A Unified Approach to Performance Analysis*. Hoboken, NJ, USA: Wiley, 2000.
[15] C. Zhong, M. Matthaiou, G. K. Karagiannidis, and T. Ratnarajah, "Generic ergodic capacity bounds for fixed-gain AF dual-hop relaying systems," *IEEE Trans. Veh. Technol.*, vol. 60, no. 8, pp. 3814–3824, Oct. 2011.
[16] F. Gao, T. Cui, and A. Nallanathan, "Optimal training design for channel estimation in decode-and-forward relay networks with individual and total power constraints," *IEEE Trans. Signal Process.*, vol. 56, no. 12, pp. 5937–5949, Dec. 2008.
[17] D. Tse and P. Viswanath, *Fundamentals of Wireless Communication*. Cambridge, U.K.: Cambridge Univ. Press, 2005.
[18] I. S. Gradshteyn and I. M. Ryzhik, *Table of Integrals, Series, and Products*, 7th ed. New York, NY, USA: Academic, 2007.
[19] F. W. Olver, D. W. Lozier, R. F. Boisvert, and C. W. Clark, *NIST Handbook of Mathematical Functions*. New York, NY, USA: Cambridge Univ. Press, 2010.

Transmit Antenna Selection in Cognitive MIMO Relaying With Multiple Primary Transceivers

Phee Lep Yeoh, *Member, IEEE*, Maged Elkashlan, *Member, IEEE*, Kyeong Jin Kim, *Senior Member, IEEE*, Trung Q. Duong, *Senior Member, IEEE*, and George K. Karagiannidis, *Fellow, IEEE*

***Abstract*—We consider transmit antenna selection (TAS) in cognitive multiple-input–multiple-output (MIMO) relay networks as an interference-aware design for secondary users (SUs) to ensure power and interference constraints of multiple primary users (PUs). In doing so, we derive new exact and asymptotic expressions for the outage probability of TAS with maximal ratio combining (TAS/MRC) and with selection combining (TAS/SC) over Rayleigh fading. The proposed analysis and simulations highlight that TAS/MRC and TAS/SC with decode-and-forward relaying achieve the same diversity order in cognitive MIMO networks, which scales with the minimum number of antennas at the SUs. Furthermore, we accurately characterize the outage gap between TAS/MRC and TAS/SC relaying as a concise ratio of their array gains.**

***Index Terms*—Cognitive radio, cooperative communications, multiple-input–multiple-output (MIMO).**

I. INTRODUCTION

Multiple-input–multiple-output (MIMO) relaying in cognitive spectrum sharing is a revolutionary framework to combat spectrum scarcity and support the dramatic expansion of wireless networks [1]. From a power perspective, cognitive MIMO relaying holds the key of addressing the conflicting demands of increased reliability for secondary users

Manuscript received February 7, 2014; revised July 14, 2014, December 1, 2014; accepted January 9, 2015. Date of publication January 15, 2015; date of current version January 13, 2016. The review of this paper was coordinated by Prof. Y. Gong. This work was presented in part at the IEEE Global Communications Conference, Atlanta, GA, December 2013.

P. L. Yeoh is with the University of Melbourne, Melbourne, VIC 3010, Australia (e-mail: phee.yeoh@unimelb.edu.au).

M. Elkashlan is with the Queen Mary, University of London, London E1 4NS, U.K. (e-mail: maged.elkashlan@eecs.qmul.ac.uk).

K. J. Kim is with the Mitsubishi Electric Research Laboratories, Cambridge, MA 02139-1955 USA (e-mail: kkim@merl.com).

T. Q. Duong is with Queen's University Belfast, Belfast BT7 1NN, U.K. (e-mail: trung.q.duong@qub.ac.uk).

G. K. Karagiannidis is with Khalifa University, Abu Dhabi 127788, UAE, and also with Aristotle University of Thessaloniki, 54124 Thessaloniki, Greece (e-mail: geokarag@auth.gr).

Color versions of one or more of the figures in this paper are available online at http://ieeexplore.ieee.org.

Digital Object Identifier 10.1109/TVT.2015.2392753

(SUs) while satisfying strict interference constraints in the primary users (PUs). However, the benefits of cognitive MIMO relaying may be constrained by the restricted power and feedback overheads of SUs. Against this backdrop, we consider transmit antenna selection (TAS) as an interference-aware design for cognitive MIMO relay networks. Specifically, we focus on underlay spectrum sharing with two low-power and low-complexity protocols: 1) TAS with receiver maximal-ratio combining (TAS/MRC); and 2) TAS with receiver selection combining (TAS/SC).

Scanning the open literature, for underlay spectrum sharing without relays, the ergodic capacity and outage probability of TAS/MRC were studied in [2] and [3], respectively. In [4], a symbol-error-rate-optimal selection rule was proposed for TAS, with a single SU receiver and a single PU receiver (PU-Rxs), whereas in [5], power allocation for TAS/MRC with a PU transmitter (PU-Tx) and a PU-Rx was analyzed. More recently, TAS in underlay spectrum sharing with decode-and-forward (DF) relaying has been examined in [6]–[8]. The ergodic capacity of TAS with a single PU-Rx was derived in [6], whereas in [7] and [8], the outage probability of TAS/MRC with multiple PU-Rxs was characterized. Finally, in [9], the results of [7] and [8] were extended to consider the impact of multiple PU-Txs on the outage probability.

In this paper, in contrast to the aforementioned works, we consider the impact of multiple PU-Txs and multiple PU-Rxs on TAS/MRC and TAS/SC relaying. This allows us to examine the joint impact of three underlay spectrum sharing power constraints on TAS/MRC and TAS/SC:

- maximum transmit power at the SU transmitters (SU-Txs) $\mathcal{P}_{\rm T}$;
- interference temperature at the PU-Rxs due to the SU-Txs $\mathcal{Q}$;
- interference power at the SU receivers (SU-Rxs) due to the PU-Txs $\mathcal{P}_{\rm I}$.

To do so, we derive new closed-form expressions for the cumulative distribution function (CDF) of the signal-to-interference ratios (SIRs) for TAS/MRC and TAS/SC relaying with multiple PU transceivers. Based on these, we present new formulas for the exact and asymptotic outage probability. Furthermore, we accurately characterize the outage gap between TAS/MRC and TAS/SC relaying as a concise ratio of their array gains.

II. System Model

We study MIMO relaying in underlay spectrum sharing networks, as shown in Fig. 1, with a SU source (S), SU relay (R), and SU destination (D) sharing the same spectrum with L PU-Txs and L PU-Rxs. According to underlay spectrum sharing rules, the interference temperature at the PU-Rxs must not exceed a predetermined threshold, $\mathcal{Q}$. As such, the transmit power with TAS at S can be constrained as

$$P_{\rm S} = \min\left(\mathcal{P}_{\rm T}, \frac{\mathcal{Q}}{\max\limits_{l\in\{1,\ldots,L\}} |h_{1i^*l}|^2}\right) \tag{1}$$

where $|\cdot|$ denotes the absolute value, and h_{1i^*l} are the channel coefficients from the selected ith transmit antenna at S to the L PU-Rxs.[1] The transmit power at R, i.e., $P_{\rm R}$, can be obtained from (1) by replacing h_{1i^*l} with the corresponding channel coefficients h_{2j^*l}, from the selected ith transmit antenna at R to the L PU-Rxs.

A. TAS/MRC Relaying

Considering TAS/MRC in the S $\rightarrow$ R link, a single transmit antenna is selected at S, and all the receive antennas at R are combined using MRC. As such, the instantaneous received SIR is

$$\tilde{\gamma}_1 = \frac{P_{\rm S}\|\mathbf{g}_{1i^*}\|^2}{\sum_{\ell=1}^{L}\mathcal{P}_{\rm I}|h_{3\ell j}|^2} \tag{2}$$

where $P_{\rm S}$ is the transmit power at S defined in (1), $\mathcal{P}_{\rm I}$ is the interference power from the L PU-Tx nodes, and $\|\cdot\|$ denotes the Euclidean norm. In (2), we define

$$\|\mathbf{g}_{1i^*}\|^2 = \max_{i\in\{1,\ldots,N_{\rm S}\}}\left\{\left\|\left[g_{1i1},\ldots,g_{1iN_{\rm R}}\right]\right\|^2\right\} \tag{3}$$

as the largest channel vector norm squared in the S $\rightarrow$ R link, whereas $|h_{3\ell j}|^2$ is the channel gain from the ℓth PU-Tx node to all the receive antennas at R. In the R $\rightarrow$ D link, a single transmit antenna is selected at R, and all the receive antennas at D are combined using MRC. As such, the instantaneous received SIR $\tilde{\gamma}_2$ can be obtained from (2) by replacing $P_{\rm S}$ with $P_{\rm R}$, and considering

$$\|\mathbf{g}_{2j^*}\|^2 = \max_{j\in\{1,\ldots,N_{\rm R}\}}\left\{\left\|\left[g_{2j1},\ldots,g_{2jN_{\rm D}}\right]\right\|^2\right\} \tag{4}$$

as the largest channel vector norm squared in the R $\rightarrow$ D link, and $|h_{4\ell k}|^2$ as the channel gain from the ℓth PU-Tx node to all the receive antennas at D. Based on $\tilde{\gamma}_1$ and $\tilde{\gamma}_2$, the SIR of the S $\rightarrow$ R $\rightarrow$ D link can be written as [10]

$$\gamma_{\rm D,TAS/MRC} = \min(\tilde{\gamma}_1, \tilde{\gamma}_2) \tag{5}$$

which is due to the fact that the end-to-end SIR is determined by the weakest link.

B. TAS/SC Relaying

Considering TAS/SC in the S $\rightarrow$ R link, a single transmit–receive antenna pair is selected at S and R such that the instantaneous received SIR is given by

$$\hat{\gamma}_1 = \frac{P_{\rm S}|g_{1i^*j^*}|^2}{\sum\limits_{\ell=1}^{L}\mathcal{P}_{\rm I}|h_{3\ell j^*}|^2}. \tag{6}$$

In (6), $|g_{1i^*j^*}|^2 = \max_{i,j}\{|g_{1ij}|^2\}$ is the largest channel gain from S to R, and $|h_{3\ell j^*}|^2$ is the channel gain from the ℓth PU-Tx node to the selected receive antenna at R. In the R $\rightarrow$ D link, a single transmit-receive antenna pair is selected at R and D such that the instantaneous received SIR $\hat{\gamma}_2$ is obtained from (6) by replacing $P_{\rm S}$ with $P_{\rm R}$ and by

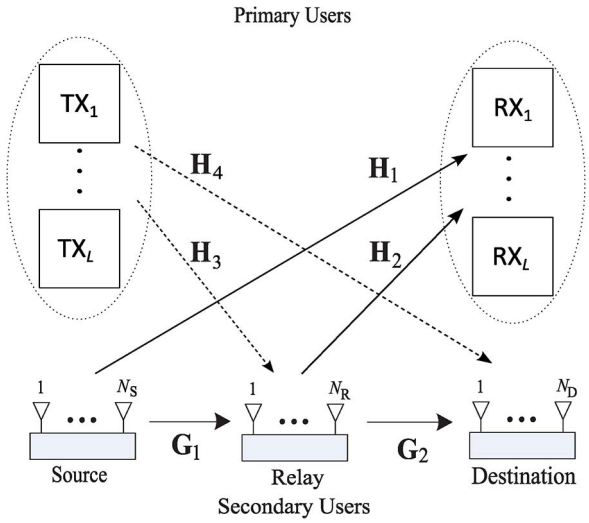

Fig. 1. Cognitive MIMO relaying network with multiple primary transceivers.

[1] We adopt the common assumption that the SUs have perfect knowledge of the channel state information (CSI) of the PU-Rxs as in [2], [3].

considering $|g_{2j^\dagger k^*}|^2 = \max_{j,k}\{|g_{2jk}|^2\}$ as the largest channel gain from R to D, and $|h_{4\ell k^*}|^2$ as the channel gain from the ℓth PU-Tx node to the selected receive antenna at D. Note that the selected receive antenna at R, i.e., j^*, may not be the same as the selected transmit antenna at R, i.e., $j^\dagger$. The SIR of the $\mathsf{S}\to\mathsf{R}\to\mathsf{D}$ link can be evaluated as

$$\gamma_{\mathrm{D,TAS/SC}} = \min(\hat{\gamma}_1, \hat{\gamma}_2). \tag{7}$$

We note that TAS/SC simply selects the strongest SU-Rx antenna resulting in lower receiver complexity relative to TAS/MRC where all the receive antennas are combined.

III. Outage Probability

The outage probability is defined as the probability that the end-to-end SIR is below a minimum threshold γ_{th} and can be written as

$$P_{\mathrm{out}} = \Pr\{\gamma_{\mathrm{D}} \le \gamma_{\mathrm{th}}\} = F_{\gamma_{\mathrm{D}}}(\gamma_{\mathrm{th}}) \tag{8}$$

where $F_{\gamma_{\mathrm{D}}}(\gamma_{\mathrm{th}})$ is the CDF of γ_{D}. Given that the end-to-end SIRs in both (5) and (7) are based on the minimum SIR in each link, the exact outage probability can be further evaluated as

$$P_{\mathrm{out}} = F_{\gamma_1}(\gamma_{\mathrm{th}}) + F_{\gamma_2}(\gamma_{\mathrm{th}}) - F_{\gamma_1}(\gamma_{\mathrm{th}})F_{\gamma_2}(\gamma_{\mathrm{th}}) \tag{9}$$

where $\gamma_1 = \tilde{\gamma}_1, \gamma_2 = \tilde{\gamma}_2$ for TAS/MRC relaying, and $\gamma_1 = \hat{\gamma}_1$, $\gamma_2 = \hat{\gamma}_2$ for TAS/SC relaying.

A. TAS/MRC Relaying

Theorem 1: The CDF of $\tilde{\gamma}_1$ for TAS/MRC in the presence of L PU-Txs and PU-Rxs is

$$F_{\tilde{\gamma}_1}(\gamma) = 1 - \epsilon_1 \sum_{n=1}^{N_\eta} \binom{N_\eta}{n} (-1)^{n+1} \left(1 + \frac{\mathcal{P}_{\mathrm{I}}\Omega_{h_3} n\gamma}{\mathcal{P}_{\mathrm{T}}\Omega_{g_1}}\right)^{-L} \Delta_1$$
$$- \sum_{n=1}^{N_\eta}\sum_{l=0}^{L-1} \frac{\binom{N_\eta}{n}\binom{L-1}{l} L(-1)^{l+n+1}}{(l+1)e^{\frac{\mathcal{Q}(l+1)}{\mathcal{P}_{\mathrm{T}}\Omega_{h_1}}}} \left(\frac{\mathcal{Q}(l+1)\Omega_{g_1}}{\mathcal{P}_{\mathrm{I}}\Omega_{h_1}\Omega_{h_3} n\gamma}\right)^{L} \Delta_2 \tag{10}$$

where

$$\Delta_1 = \prod_{p=1}^{N_{\mathrm{R}}-1} \left[\sum_{n_p=0}^{n_{p-1}} \binom{n_{p-1}}{n_p} \left(\frac{1}{p}\right)^{n_p - n_{p+1}}\right] \times \frac{\Gamma\left(L+\sigma_{n_p}\right)}{\Gamma(L)} \left(\frac{\mathcal{P}_{\mathrm{T}}\Omega_{g_1}}{\mathcal{P}_{\mathrm{I}}\Omega_{h_3}\gamma} + n\right)^{-\sigma_{n_p}} \tag{11}$$

$$\Delta_2 = \prod_{p=1}^{N_{\mathrm{R}}-1} \left[\sum_{n_p=0}^{n_{p-1}} \binom{n_{p-1}}{n_p} \left(\frac{1}{p!}\right)^{n_p - n_{p+1}}\right] \left(\frac{1}{n}\right)^{\sigma_{n_p}} \times \frac{\Gamma\left(L+\sigma_{n_p}\right)\Gamma\left(1+\sigma_{n_p}\right)}{\Gamma(L)} \sum_{\alpha=0}^{\sigma_{n_p}} \frac{1}{\alpha!} \left(\frac{\mathcal{Q}(l+1)}{\mathcal{P}_{\mathrm{T}}\Omega_{h_1}}\right)^{\alpha} \times \Psi\left(\sigma_{n_p}+L, \alpha+L; \frac{\mathcal{Q}(l+1)}{\mathcal{P}_{\mathrm{T}}\Omega_{h_1}} + \frac{\mathcal{Q}(l+1)\Omega_{g_1}}{\mathcal{P}_{\mathrm{I}}\Omega_{h_1} n\gamma\Omega_{h_3}}\right) \tag{12}$$

and $\epsilon_1 = (1 - e^{-(\mathcal{Q}/\mathcal{P}_{\mathrm{T}}\Omega_{h_1})})^L$, $N_\eta = N_{\mathsf{S}}$, $\sigma_{n_p} = \sum_{p=1}^{N_{\mathrm{R}}-1} n_p$, $n_0 = n$, and $n_{N_R} = 0$. The symbol $\Gamma(\cdot)$ in (11) and (12) represents the gamma function [11, Eq. (8.310.1)], and $\Psi(a,b;z)$ is the confluent hypergeometric function [11, Eq. (9.210.2)]. The parameters Ω_{g_1}, Ω_{h_1}, and Ω_{h_3} are the mean power of the Rayleigh distributed channel gains, in $\mathbf{G}_1$, $\mathbf{H}_1$, and $\mathbf{H}_3$, respectively.

Proof: See Appendix A. ■

Note that the CDF expression for TAS/MRC in (10) is consisted of easy-to-evaluate finite summations of standard functions, available in popular numerical software such as MATLAB and Mathematica. Now, given that the channels are independent, the exact CDF of $\tilde{\gamma}_2$ can be derived by simply exchanging the parameters $\Omega_{h_1} \to \Omega_{h_2}$, $\Omega_{h_3} \to \Omega_{h_4}$, $\Omega_{g_1} \to \Omega_{g_2}$, $N_{\mathrm{S}} \to N_{\mathrm{R}}$, and $N_{\mathrm{R}} \to N_{\mathrm{D}}$.

B. TAS/SC Relaying

Theorem 2: The CDF of $\hat{\gamma}_1$ for TAS/SC in the presence of L PU-Txs and PU-Rxs is

$$F_{\hat{\gamma}_1}(\gamma) = 1 - \epsilon_1 \sum_{n=1}^{N_\eta} \binom{N_\eta}{n} (-1)^{n+1} \left(1 + \frac{\mathcal{P}_{\mathrm{I}}\Omega_{h_3} n\gamma}{\mathcal{P}_{\mathrm{T}}\Omega_{g_1}}\right)^{-L}$$
$$- \sum_{n=1}^{N_\eta}\sum_{l=0}^{L-1} \frac{\binom{N_\eta}{n}\binom{L-1}{l} L(-1)^{l+n+1}}{(l+1)e^{\frac{\mathcal{Q}(l+1)}{\mathcal{P}_{\mathrm{T}}\Omega_{h_1}}}} \left(\frac{\mathcal{Q}(l+1)\Omega_{g_1}}{\mathcal{P}_{\mathrm{I}}\Omega_{h_1}\Omega_{h_3} n\gamma}\right)^{L} \Delta_3 \tag{13}$$

where

$$\Delta_3 = e^{\frac{\mathcal{Q}(l+1)}{\mathcal{P}_{\mathrm{T}}\Omega_{h_1}} + \frac{\mathcal{Q}(l+1)\Omega_{g_1}}{\mathcal{P}_{\mathrm{I}}\Omega_{h_1}\Omega_{h_3} n\gamma}} \times \Gamma\left(1-L, \frac{\mathcal{Q}(l+1)}{\mathcal{P}_{\mathrm{T}}\Omega_{h_1}} + \frac{\mathcal{Q}(l+1)\Omega_{g_1}}{\mathcal{P}_{\mathrm{I}}\Omega_{h_1}\Omega_{h_3} n\gamma}\right) \tag{14}$$

with $N_\eta = N_{\mathsf{S}}N_{\mathsf{R}}$, and $\Gamma(\cdot,\cdot)$ being the upper incomplete gamma function [11, Eq. (8.350.2)].

Proof: See Appendix B. ■

The exact CDF of $\hat{\gamma}_2$ follows directly by exchanging the parameters $\Omega_{h_1} \to \Omega_{h_2}$, $\Omega_{h_3} \to \Omega_{h_4}$, $\Omega_{g_1} \to \Omega_{g_2}$, $N_{\mathrm{S}} \to N_{\mathrm{R}}$, and $N_{\mathrm{R}} \to N_{\mathrm{D}}$, in (13). Interestingly, we observe that (13) can be obtained directly from (10), by setting $N_\eta = N_{\mathsf{S}}N_{\mathsf{R}}$, $\Delta_1 = 1$, and $\Delta_2 = \Delta_3$.

IV. Asymptotic Outage Probability

To obtain further insights, we examine the asymptotic outage probability of TAS/MRC and TAS/SC relaying, when $\mathcal{P}_{\mathrm{T}} \to \infty$. Due to the fact that the CDFs of γ_{D} in (5) and (7) are both constrained by the lower diversity link, the asymptotic outage probability can be evaluated as

$$P_{\mathrm{out}}^{\infty} = \begin{cases} F_{\gamma_1}^{\infty}(\gamma_{\mathrm{th}}) & N_{\mathrm{S}}N_{\mathrm{R}} < N_{\mathrm{R}}N_{\mathrm{D}} \\ F_{\gamma_2}^{\infty}(\gamma_{\mathrm{th}}) & N_{\mathrm{S}}N_{\mathrm{R}} > N_{\mathrm{R}}N_{\mathrm{D}} \\ F_{\gamma_1}^{\infty}(\gamma_{\mathrm{th}}) + F_{\gamma_2}^{\infty}(\gamma_{\mathrm{th}}) & N_{\mathrm{S}}N_{\mathrm{R}} = N_{\mathrm{R}}N_{\mathrm{D}} \end{cases} \tag{15}$$

where $\gamma_1 = \tilde{\gamma}_1, \gamma_2 = \tilde{\gamma}_2$ for TAS/MRC, and $\gamma_1 = \hat{\gamma}_1, \gamma_2 = \hat{\gamma}_2$ for TAS/SC.

A. TAS/MRC Relaying

Theorem 3: A closed-form expression for the asymptotic CDF of $\tilde{\gamma}_1$ is

$$F_{\tilde{\gamma}_1}^{\infty}(\gamma) = \Phi_1 \left(\frac{\gamma\mathcal{P}_{\mathrm{I}}}{\mathcal{P}_{\mathrm{T}}}\right)^{N_{\mathrm{S}}N_{\mathrm{R}}} + \Phi_2 \left(\frac{\gamma\mathcal{P}_{\mathrm{I}}}{\mathcal{Q}}\right)^{N_{\mathrm{S}}N_{\mathrm{R}}} \tag{16}$$

where

$$\Phi_1 = \frac{\epsilon_1\Gamma(N_{\mathrm{S}}N_{\mathrm{R}}+L)\Omega_{h_3}^{N_{\mathrm{S}}N_{\mathrm{R}}}}{(\Gamma(N_{\mathrm{R}}+1))^{N_{\mathrm{S}}}\Gamma(L)\Omega_{g_1}^{N_{\mathrm{S}}N_{\mathrm{R}}}} \tag{17}$$

$$\Phi_2 = \sum_{l=0}^{L-1} \frac{\binom{L-1}{l}(-1)^l L\Gamma(N_{\mathrm{S}}N_{\mathrm{R}}+L)(\Omega_{h_1}\Omega_{h_3})^{N_{\mathrm{S}}N_{\mathrm{R}}}}{(\Gamma(N_{\mathrm{R}}+1))^{N_{\mathrm{S}}}\Gamma(L)(l+1)^{N_{\mathrm{S}}N_{\mathrm{R}}+1}\Omega_{g_1}^{N_{\mathrm{S}}N_{\mathrm{R}}}} \times \Gamma\left(N_{\mathrm{S}}N_{\mathrm{R}}+1, \frac{\mathcal{Q}(l+1)}{\mathcal{P}_{\mathrm{T}}\Omega_{h_1}}\right). \tag{18}$$

Proof: See Appendix C. ■

Note that (16) accurately captures the separable contributions of $\mathcal{P}_{\mathrm{T}}$, $\mathcal{Q}$, and $\mathcal{P}_{\mathrm{I}}$ on the statistics of $\tilde{\gamma}_1$ as $\mathcal{P}_{\mathrm{T}} \to \infty$. The accuracy of our asymptotic approximation is corroborated by simulation results in Section VI. The asymptotic CDF of $\tilde{\gamma}_2$ follows directly from (16) with a change of variables.

B. TAS/SC Relaying

Theorem 4: A closed-form expression for the asymptotic CDF of $\hat{\gamma}_1$ is given by

$$F^{\infty}_{\hat{\gamma}_1}(\gamma) = \Phi_1 \left(\Gamma(N_{\mathrm{R}}+1)\right)^{N_{\mathrm{S}}} \left(\frac{\gamma \mathcal{P}_{\mathrm{I}}}{\mathcal{P}_{\mathrm{T}}}\right)^{N_{\mathrm{S}}N_{\mathrm{R}}} + \Phi_2 \left(\Gamma(N_{\mathrm{R}}+1)\right)^{N_{\mathrm{S}}} \left(\frac{\gamma \mathcal{P}_{\mathrm{I}}}{\mathcal{Q}}\right)^{N_{\mathrm{S}}N_{\mathrm{R}}} \quad (19)$$

where Φ_1 and Φ_2 are defined in (17) and (18), respectively.

Proof: See Appendix D. ■

Comparing (19) and (16), we can infer that the asymptotic outage probability of TAS/MRC is lower than that of TAS/SC. The asymptotic CDF of $\hat{\gamma}_1$ can be obtained from (19) by applying a change of variables.

C. Comparison of TAS/MRC and TAS/SC

For $\mathcal{Q} = \mu \mathcal{P}_{\mathrm{T}}$, the asymptotic outage probability in (15) based on (16) and (19) can be written as

$$P^{\infty}_{\mathrm{out}} = \left(\mathcal{O}_A \mathcal{P}_{\mathrm{T}}\right)^{-\mathcal{O}_D} + o\left(\mathcal{P}_{\mathrm{T}}^{-\mathcal{O}_D}\right) \quad (20)$$

where $\mathcal{O}_D$ is the diversity order, and $\mathcal{O}_A$ is the array gain.

Inspecting (19) and (16), it is evident that TAS/MRC and TAS/SC relaying achieve the same diversity order of $\mathcal{O}_D = \min(N_{\mathrm{S}}N_{\mathrm{R}}, N_{\mathrm{R}}N_{\mathrm{D}})$. Given the same diversity order, the outage gap between the two protocols can be concisely expressed as a ratio of their respective array gains as

$$\frac{\mathcal{O}_{A,\mathrm{TAS/MRC}}}{\mathcal{O}_{A,\mathrm{TAS/SC}}} = \begin{cases} \left(\Gamma(N_{\mathrm{R}}+1)\right)^{\frac{1}{N_{\mathrm{R}}}} & N_{\mathrm{S}}N_{\mathrm{R}} < N_{\mathrm{R}}N_{\mathrm{D}} \\ \left(\Gamma(N_{\mathrm{D}}+1)\right)^{\frac{1}{N_{\mathrm{D}}}} & N_{\mathrm{S}}N_{\mathrm{R}} > N_{\mathrm{R}}N_{\mathrm{D}} \\ \left(\frac{\Theta_1 (\Gamma(N_{\mathrm{R}}+1))^{\frac{1}{N_{\mathrm{R}}}} + \Theta_2 (\Gamma(N_{\mathrm{D}}+1))^{\frac{1}{N_{\mathrm{D}}}}}{\Theta_1+\Theta_2}\right)^{\frac{1}{N_{\mathrm{S}}N_{\mathrm{R}}}} & N_{\mathrm{S}}N_{\mathrm{R}} = N_{\mathrm{R}}N_{\mathrm{D}} \end{cases} \quad (21)$$

where

$$\Theta_1 = \frac{\epsilon_1 \Gamma(N_{\mathrm{S}}N_{\mathrm{R}}+L)\Omega_{h3}^{N_{\mathrm{S}}N_{\mathrm{R}}}}{\left(\Gamma(N_{\mathrm{R}}+1)\right)^{N_{\mathrm{S}}} \Gamma(L) \Omega_{g1}^{N_{\mathrm{S}}N_{\mathrm{R}}}} + \sum_{l=0}^{L-1} \frac{\binom{L-1}{l}(-1)^l L \Gamma(N_{\mathrm{S}}N_{\mathrm{R}}+L) \left(\Omega_{h_1}\Omega_{h_3}\right)^{N_{\mathrm{S}}N_{\mathrm{R}}}}{\left(\Gamma(N_{\mathrm{R}}+1)\right)^{N_{\mathrm{S}}} \Gamma(L)(l+1)^{N_{\mathrm{S}}N_{\mathrm{R}}+1} \left(\mu\Omega_{g_1}\right)^{N_{\mathrm{S}}N_{\mathrm{R}}}} \times \Gamma\left(N_{\mathrm{S}}N_{\mathrm{R}}+1, \frac{\mu(l+1)}{\Omega_{h_1}}\right) \quad (22)$$

$$\Theta_2 = \frac{\epsilon_2 \Gamma(N_{\mathrm{R}}N_{\mathrm{D}}+L)\Omega_{h_4}^{N_{\mathrm{R}}N_{\mathrm{D}}}}{\left(\Gamma(N_{\mathrm{D}}+1)\right)^{N_{\mathrm{R}}} \Gamma(L) \Omega_{g2}^{N_{\mathrm{R}}N_{\mathrm{D}}}} + \sum_{l=0}^{L-1} \frac{\binom{L-1}{l}(-1)^l L \Gamma(N_{\mathrm{R}}N_{\mathrm{D}}+L) \left(\Omega_{h_2}\Omega_{h_4}\right)^{N_{\mathrm{R}}N_{\mathrm{D}}}}{\left(\Gamma(N_{\mathrm{D}}+1)\right)^{N_{\mathrm{R}}} \Gamma(L)(l+1)^{N_{\mathrm{R}}N_{\mathrm{D}}+1} \left(\mu\Omega_{g_2}\right)^{N_{\mathrm{R}}N_{\mathrm{D}}}} \times \Gamma\left(N_{\mathrm{R}}N_{\mathrm{D}}+1, \frac{\mu(l+1)}{\Omega_{h_2}}\right). \quad (23)$$

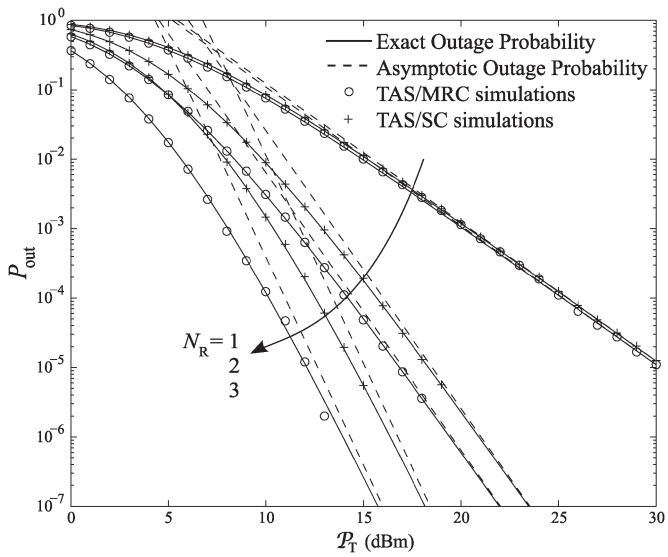

Fig. 2. Outage probability of TAS/MRC and TAS/SC relaying with $L = 3$, $N_{\mathrm{S}} = N_{\mathrm{D}} = 2$, $\mathcal{Q} = 2\mathcal{P}_{\mathrm{T}}$, and $\mathcal{P}_{\mathrm{I}} = 5$ dBm.

Interestingly, we note that, although the array gains of TAS/MRC and TAS/SC relaying decrease with increasing $\mathcal{P}_{\mathrm{I}}$, the outage gap between the two protocols is independent of $\mathcal{P}_{\mathrm{I}}$.

V. Numerical Examples

We consider a simple 2-D topology with the PU-Tx cluster centered at (0,1), the PU-Rx cluster centered at (1, 1), S at (0,0), D at (1,0), and R at $(0, d_{\mathrm{R}})$ with $0 < d_{\mathrm{R}} < 1$. The channel gains are nonidentical Rayleigh distributed random variables with average channel power values, Ω_{g1}, Ω_{g2}, Ω_{h1}, Ω_{h2}, Ω_{h3}, and Ω_{h4}, defined according to an exponential-decay path-loss model of $d^{-\nu}$, where d is the distance between a given pair of transceivers, and $\nu = 3$ is the path-loss coefficient. In all the figures, we use '$\circ$' to denote simulation points for TAS/MRC and '$+$' to denote simulation points for TAS/SC. The solid curves represent the exact outage probability, and the dashed curves represent the asymptotic outage probability. We observe good agreement between our analytical results and simulations in all the plots.

Figs. 2 and 3 plot the outage probability versus $\mathcal{P}_{\mathrm{T}}$. The outage threshold is set to $\gamma_{\mathrm{th}} = 5$ dB, and the interference power is $\mathcal{P}_{\mathrm{I}} = 5$ dBm. Fig. 2 plots the outage probability when $\mathcal{Q}$ is proportional to $\mathcal{P}_{\mathrm{T}}$, according to $\mathcal{Q} = 2\mathcal{P}_{\mathrm{T}}$, which represents the scenario where the SU transmit power values are not severely constrained by $\mathcal{Q}$. We observe that the outage probability of TAS/MRC and TAS/SC improves continuously with increasing $\mathcal{P}_{\mathrm{T}}$ without any outage floor. We also note that the outage probability improves significantly with increasing N_{R}. As expected, TAS/MRC relaying offers a lower outage probability relative to TAS/SC relaying. Fig. 3 plots the outage probability for the case where $\mathcal{Q}$ is fixed and independent of $\mathcal{P}_{\mathrm{T}}$, which represents the scenario where the SU transmit power level are strictly limited by $\mathcal{Q}$ as $\mathcal{P}_{\mathrm{T}}$ grows large. As such, the outage probability does not continuously decrease with increasing $\mathcal{P}_{\mathrm{T}}$. We observe that our analytical curves accurately predict the outage floor in the high $\mathcal{P}_{\mathrm{T}}$ regime. We note that the outage probability increases with increasing number of PUs L.

Figs. 4 and 5 plot the outage probability versus d_{R} with $\mathcal{P}_{\mathrm{T}} = 10$ dBm, $\mathcal{Q} = 20$ dBm, $\mathcal{P}_{\mathrm{I}} = 5$ dBm, and $\gamma_{\mathrm{th}} = 5$ dB. Fig. 4 plots the outage probability for different PU-TxRx cluster locations. As expected, the outage probability decreases when the PU-TxRx clusters are located farther away from the SUs. Interestingly, the relay location

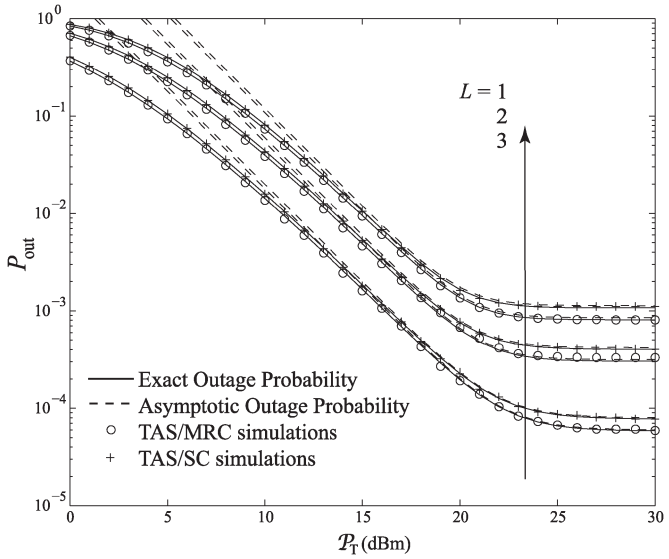

Fig. 3. Outage probability of TAS/MRC and TAS/SC relaying with $N_{\text{S}} = N_{\text{D}} = 2$, $N_{\text{R}} = 1$, $\mathcal{Q} = 20$ dBm, and $\mathcal{P}_{\text{I}} = 5$ dBm.

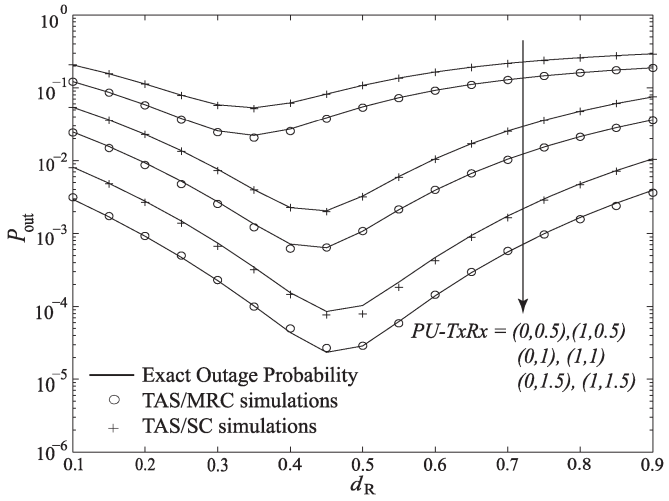

Fig. 4. Outage probability of TAS/MRC and TAS/SC relaying with $N_{\text{S}} = N_{\text{R}} = N_{\text{D}} = 2$, and $L = 2$.

corresponding to the minimum outage probability is closer to the source when the PU-TxRx clusters are closer to the SUs. Fig. 5 plots the outage probability when the PU-Txs are at (0,1) and the PU-Rxs are at (1,1). We find that an increase in N_{S} has a more prominent impact on the outage probability when the relay is located away from the source. Furthermore, we observe that the relay location corresponding to the minimum outage probability is closer to the destination when N_{S} increases from 1 to 3.

VI. Conclusion

We have examined TAS/MRC and TAS/SC with DF relaying in underlay spectrum sharing with multiple PU transceivers and multiple antennas at the SUs. New analytical expressions have been derived for the exact and asymptotic outage probability of TAS/MRC and TAS/SC in the presence of L primary transceivers. Our analysis and simulations highlight that TAS/MRC and TAS/SC with DF relaying achieve the same diversity order when $\mathcal{Q}$ is directly proportional to $\mathcal{P}_{\text{T}}$. These results are instrumental for limited-feedback beamforming as a promising extension to this paper.

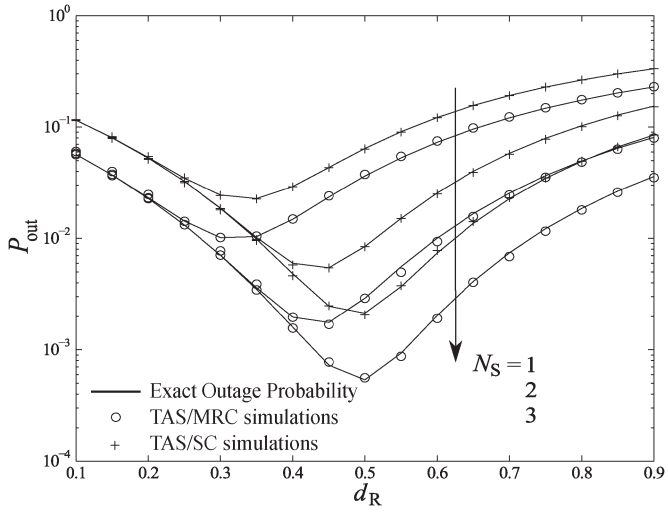

Fig. 5. Outage probability of TAS/MRC and TAS/SC relaying with $N_{\text{R}} = N_{\text{D}} = 2$, $L = 3$, and PU-TxRx $= (0,1), (1,1)$.

Appendix A
Proof of Theorem 1

The CDF of $\tilde{\gamma}_1$ conditioned on $Z_1 = \sum_{\ell=1}^{L} \mathcal{P}_{\text{I}} \|\mathbf{h}_{3\ell}\|^2$ can be derived as

$$F_{\tilde{\gamma}_1|Z_1}(\gamma) = \underbrace{F_{X_1}\left(\frac{\gamma Z_1}{\mathcal{P}_{\text{T}}}\right) F_{Y_1}\left(\frac{\mathcal{Q}}{\mathcal{P}_{\text{T}}}\right)}_{\mathcal{I}_1(Z_1)} + \underbrace{\int_{\frac{\mathcal{Q}}{\mathcal{P}_{\text{T}}}}^{\infty} f_{Y_1}(y) F_{X_1}\left(\frac{y\gamma Z_1}{\mathcal{Q}}\right) dy}_{\mathcal{I}_2(Z_1)}. \tag{24}$$

where $F_{Y_1}(x) = (1 - e^{-(x/\Omega_{h_1})})^L$ is the CDF of $Y_1 = \max_{l=1,\ldots,L} |h_{1i^*l}|^2$ with corresponding probability density function (PDF) $f_{Y_1}(y) = (L/\Omega_{h_1}) \sum_{l=0}^{L-1} \binom{L-1}{l} (-1)^l e^{-y((l+1)/\Omega_{h_1})}$, and

$$F_{X_1}(x) = 1 - \sum_{n=1}^{N_{\text{S}}} \binom{N_{\text{S}}}{n} (-1)^{n+1} e^{-\frac{nx}{\Omega_{g_1}}} \left(\sum_{p=0}^{N_{\text{R}}-1} \frac{\left(\frac{x}{\Omega_{g_1}}\right)^p}{p!} \right)^n \tag{25}$$

is the CDF of $X_1 = \|\mathbf{g}_{1i^*}\|^2$. Integrating $\mathcal{I}_1(Z_1)$ over the PDF of Z_1, i.e., $f_{Z_1}(x) = (x^{L-1} e^{-(x/\mathcal{P}_{\text{I}}\Omega_{h_3})})/\Gamma(L)(\mathcal{P}_{\text{I}}\Omega_{h_3})^L$, results in

$$\begin{aligned} \mathbb{E}_{Z_1}\{\mathcal{I}_1(Z_1)\} &= F_{Y_1}\left(\frac{\mathcal{Q}}{\mathcal{P}_{\text{T}}}\right) - F_{Y_1}\left(\frac{\mathcal{Q}}{\mathcal{P}_{\text{T}}}\right) \sum_{n=1}^{N_{\text{S}}} \binom{N_{\text{S}}}{n} \frac{(-1)^{n+1}}{(\mathcal{P}_{\text{I}}\Omega_{h_3})^L} \\ &\times \prod_{p=1}^{N_{\text{R}}-1} \left[\sum_{n_p=0}^{n_{p-1}} \binom{n_{p-1}}{n_p} \left(\frac{1}{p}\right)^{n_p - n_{p+1}} \right] \left(\frac{\gamma}{\mathcal{P}_{\text{T}}\Omega_{g_1}} \right)^{\sum_{p=1}^{N_{\text{R}}-1} n_p} \\ &\times \frac{\Gamma\left(L + \sum_{p=1}^{N_{\text{R}}-1} n_p\right)}{\Gamma(L)} \left(\frac{n\gamma}{\mathcal{P}_{\text{T}}\Omega_{g_1}} + \frac{1}{\mathcal{P}_{\text{I}}\Omega_{h_3}} \right)^{-L - \sum_{p=1}^{N_{\text{R}}-1} n_p} \end{aligned} \tag{26}$$

where we expand the power sum according to

$$\left[\sum_{n=0}^{N-1} \frac{x^n}{n!} \right]^a = \prod_{n=1}^{N-1} \left[\sum_{a_n=0}^{a_{n-1}} \binom{a_{n-1}}{a_n} \left(\frac{1}{n!}\right)^{a_n - a_{n+1}} \right] x^{\sum_{n=1}^{N-1} a_n} \tag{27}$$

with $N>1$, $a_0=a$, and $a_N=0$. The second term $\mathcal{I}_2(Z_1)$ in (24) is evaluated as

$$\mathcal{I}_2(Z_1)=1-F_{Y_1}\left(\frac{\mathcal{Q}}{\mathcal{P}_{\rm T}}\right)-\sum_{l=0}^{L-1}\sum_{n=1}^{N_{\rm S}}\frac{\binom{L-1}{l}\binom{N_{\rm S}}{n}L(-1)^{l+n+1}}{\Omega_{h_1}} \times\prod_{p=1}^{N_{\rm R}-1}\left[\sum_{n_p=0}^{n_{p-1}}\binom{n_{p-1}}{n_p}\left(\frac{1}{p!}\right)^{n_p-n_{p+1}}\right]\left(\frac{\gamma Z_1}{\mathcal{Q}\Omega_{g_1}}\right)^{\sum_{p=1}^{N_{\rm R}-1}n_p} \times\left(\frac{l+1}{\Omega_{h_1}}+\frac{n\gamma Z_1}{\Omega_{g_1}\mathcal{Q}}\right)^{-1-\sum_{p=1}^{N_{\rm R}-1}n_p} \times\Gamma\left(1+\sum_{p=1}^{N_{\rm R}-1}n_p,\frac{(l+1)\mathcal{Q}}{\Omega_{h_1}\mathcal{P}_{\rm T}}+\frac{n\gamma Z_1}{\Omega_{g_1}\mathcal{P}_{\rm T}}\right) \quad (28)$$

where we solve the resulting integral by applying [11, 3.351.2]. Integrating $\mathcal{I}_2(Z_1)$ with respect to $f_{Z_1}(x)$ results in

$$\mathbb{E}_{Z_1}\left\{\mathcal{I}_2(Z_1)\right\}=1-F_{Y_1}\left(\frac{\mathcal{Q}}{\mathcal{P}_{\rm T}}\right)-\sum_{l=0}^{L-1}\sum_{n=1}^{N_{\rm S}}\frac{\binom{L-1}{l}\binom{N_{\rm S}}{n}L}{\left(\mathcal{P}_{\rm I}\Omega_{h_3}\right)^L\Omega_{h_1}} \times(-1)^{l+n+1}\prod_{p=1}^{N_{\rm R}-1}\left[\sum_{n_p=0}^{n_{p-1}}\binom{n_{p-1}}{n_p}\left(\frac{1}{p!}\right)^{n_p-n_{p+1}}\right]e^{-\frac{(l+1)\mathcal{Q}}{\Omega_{h_1}\mathcal{P}_{\rm T}}} \times\left(\frac{\gamma}{\mathcal{Q}\Omega_{g_1}}\right)^{\sum_{p=1}^{N_{\rm R}-1}n_p}\frac{\Gamma\left(1+\sum_{p=1}^{N_{\rm R}-1}n_p\right)\Gamma\left(\sum_{p=1}^{N_{\rm R}-1}n_p+L\right)}{\Gamma(L)} \times\sum_{\alpha=0}^{\sum_{p=1}^{N_{\rm R}-1}n_p}\frac{1}{\alpha!}\left(\frac{l+1}{\Omega_{h_1}}\right)^{\alpha+L-1}\left(\frac{\mathcal{Q}}{\mathcal{P}_{\rm T}}\right)^{\alpha}\left(\frac{\Omega_{g_1}\mathcal{Q}}{n\gamma}\right)^{\sum_{p=1}^{N_{\rm R}-1}n_p+L} \times\Psi\left(\sum_{p=1}^{N_{\rm R}-1}n_p+L,\alpha+L;\frac{(l+1)\mathcal{Q}}{\mathcal{P}_{\rm T}\Omega_{h_1}}+\frac{(l+1)\Omega_{g_1}\mathcal{Q}}{\Omega_{h_1}n\gamma\mathcal{P}_{\rm I}\Omega_{h_3}}\right). \quad (29)$$

where we solve the resulting integral using [11, 8.352/2] and [11, 9.211.4]. Finally, the exact CDF of $\tilde{\gamma}_1$ is the sum of (26) and (29), which completes the proof.

Appendix B
Proof of Theorem 2

The CDF of $\hat{\gamma}_1$ conditioned on $\hat{Z}_1=\sum_{\ell=1}^{L}\mathcal{P}_{\rm I}|h_{3\ell j^*}|^2$ is derived as

$$F_{\hat{\gamma}_1|Z_1}(\gamma)=\underbrace{F_{\hat{X}_1}\left(\frac{\gamma\hat{Z}_1}{\mathcal{P}_{\rm T}}\right)F_{Y_1}\left(\frac{\mathcal{Q}}{\mathcal{P}_{\rm T}}\right)}_{\mathcal{I}_3(\hat{Z}_1)}+\underbrace{\int_{\frac{\mathcal{Q}}{\mathcal{P}_{\rm T}}}^{\infty}f_{Y_1}(y)F_{\hat{X}_1}\left(\frac{y\gamma\hat{Z}_1}{\mathcal{Q}}\right)dy}_{\mathcal{I}_4(\hat{Z}_1)} \quad (30)$$

where $F_{\hat{X}_1}(x)=(1-e^{-(x/\Omega_{g_1})})^{N_{\rm S}N_{\rm R}}$ is the CDF of $\hat{X}_1=|g_{1i^*j^*}|^2$. We note that the PDF of $\hat{Z}_1$ is the same as that of Z_1 in Appendix A due to the fact that the SU-Rx does not coherently combine the interference signals from the PU-Txs. The remainder of the proof follows similar steps to that in Appendix A and is omitted due to space limitation.

Appendix C
Proof of Theorem 3

Approximating $\mathcal{I}_1(Z_1)$ in (24) as $\mathcal{P}_{\rm T}\to\infty$ and integrating over the PDF of Z_1 results in

$$\mathbb{E}_{Z_1}\left\{\mathcal{I}_1(Z_1)\right\}\overset{\mathcal{P}_{\rm T}\to\infty}{\approx}\frac{\epsilon_1\left(\frac{\gamma\mathcal{P}_{\rm I}\Omega_{h_3}}{\mathcal{P}_{\rm T}\Omega_{g_1}}\right)^{N_{\rm S}N_{\rm R}}\Gamma(N_{\rm S}N_{\rm R}+L)}{\left(\Gamma(N_{\rm R}+1)\right)^{N_{\rm S}}\Gamma(L)} \quad (31)$$

where $\epsilon_1=F_{Y_1}(\mathcal{Q}/\mathcal{P}_{\rm T})$, and we solve the integral according to [11, 3.326.2]. The second term $\mathcal{I}_2(Z_1)$ in (24) can be evaluated for $\mathcal{P}_{\rm T}\to\infty$ by applying a change of variables $y=(\mathcal{Q}/\mathcal{P}_{\rm T})t$ and deriving the Taylor series expansion for the CDF of X_1 in (25) as $\mathcal{P}_{\rm T}\to\infty$, which results in

$$\mathcal{I}_2(Z_1)\overset{\mathcal{P}_{\rm T}\to\infty}{\approx}\sum_{l=0}^{L-1}\frac{\binom{L-1}{l}(-1)^lL\left(\frac{\gamma Z_1\Omega_{h_1}}{\mathcal{Q}\Omega_{g_1}}\right)^{N_{\rm S}N_{\rm R}}}{(l+1)^{N_{\rm S}N_{\rm R}+1}\left(\Gamma(N_{\rm R}+1)\right)^{N_{\rm S}}} \times\Gamma\left(N_{\rm S}N_{\rm R}+1,\frac{\mathcal{Q}(l+1)}{\mathcal{P}_{\rm T}\Omega_{h_1}}\right) \quad (32)$$

where $\Gamma(\cdot,\cdot)$ denotes the upper incomplete gamma function [11, Eq. (8.350.2)], and we solve the resulting integral using [11, 3.351/2]. Integrating (32) over the PDF of Z_1 results in

$$\mathbb{E}_{Z_1}\left\{\mathcal{I}_2(Z_1)\right\}\overset{\mathcal{P}_{\rm T}\to\infty}{\approx}\sum_{l=0}^{L-1}\frac{\binom{L-1}{l}(-1)^lL}{\left(\Gamma(N_{\rm R}+1)\right)^{N_{\rm S}}}\left(\frac{\gamma\Omega_{h_1}\mathcal{P}_{\rm I}\Omega_{h_3}}{\mathcal{Q}\Omega_{g_1}}\right)^{N_{\rm S}N_{\rm R}} \times\frac{\Gamma(N_{\rm S}N_{\rm R}+L)}{\Gamma(L)(l+1)^{N_{\rm S}N_{\rm R}+1}}\Gamma\left(N_{\rm S}N_{\rm R}+1,\frac{\mathcal{Q}(l+1)}{\mathcal{P}_{\rm T}\Omega_{h_1}}\right). \quad (33)$$

Finally, the asymptotic CDF of $\tilde{\gamma}_1$ is the sum of (31) and (33), which completes the proof.

Appendix D
Proof of Theorem 4

Approximating $\mathcal{I}_3(\hat{Z}_1)$ in (30) as $\mathcal{P}_{\rm T}\to\infty$ and integrating over the PDF of $\hat{Z}_1$ result in

$$\mathbb{E}_{\hat{Z}_1}\left\{\mathcal{I}_3(\hat{Z}_1)\right\}\overset{\mathcal{P}_{\rm T}\to\infty}{\approx}\frac{\epsilon_1\Gamma(N_{\rm S}N_{\rm R}+L)}{\Gamma(L)}\left(\frac{\gamma\mathcal{P}_{\rm I}\Omega_{h_3}}{\mathcal{P}_{\rm T}\Omega_{g_1}}\right)^{N_{\rm S}N_{\rm R}}. \quad (34)$$

Applying a change of variables $dy=(\mathcal{Q}/\mathcal{P}_{\rm T})dt$ to $\mathcal{I}_4(\hat{Z}_1)$ in (30) and deriving the Taylor series expansion to the CDF of $\hat{X}_1$ as $\mathcal{P}_{\rm T}\to\infty$ results in

$$\mathcal{I}_4(\hat{Z}_1)\overset{\mathcal{P}_{\rm T}\to\infty}{\approx}\sum_{l=0}^{L-1}\binom{L-1}{l}\frac{(-1)^lL}{(l+1)^{N_{\rm S}N_{\rm R}+1}}\left(\frac{\gamma\hat{Z}_1\Omega_{h_1}}{\mathcal{Q}\Omega_{g_1}}\right)^{N_{\rm S}N_{\rm R}} \times\Gamma\left(N_{\rm S}N_{\rm R}+1,\frac{(l+1)\mathcal{Q}}{\Omega_{h_1}\mathcal{P}_{\rm T}}\right). \quad (35)$$

Integrating (35) with respect to the PDF of Z_1 results in

$$\mathbb{E}_{\hat{Z}_1}\left\{\mathcal{I}_4(\hat{Z}_1)\right\}\overset{\mathcal{P}_{\rm T}\to\infty}{\approx}\sum_{l=0}^{LN_{\rm Q}-1}\frac{\binom{L-1}{l}(-1)^lL\Gamma(N_{\rm S}N_{\rm R}+L)}{\Gamma(L)(l+1)^{N_{\rm S}N_{\rm R}+1}} \times\Gamma\left(N_{\rm S}N_{\rm R}+1,\frac{(l+1)\mathcal{Q}}{\Omega_{h_1}\mathcal{P}_{\rm T}}\right)\left(\frac{\gamma\Omega_{h_1}\mathcal{P}_{\rm I}\Omega_{h_3}}{\mathcal{Q}\Omega_{g_1}}\right)^{N_{\rm S}N_{\rm R}}. \quad (36)$$

Finally, the asymptotic CDF of $\hat{\gamma}_1$ is the sum of (34) and (36) which completes the proof.

ACKNOWLEDGMENT

The authors would like to thank the anonymous reviewers for their valuable and professional comments, which have greatly improved the quality of this paper.

REFERENCES

[1] J. Mietzner, L. Lampe, and R. Schober, "Distributed transmit power allocation for multihop cognitive-radio systems," *IEEE Trans. Wireless Commun.*, vol. 8, no. 10, pp. 5187–5201, Oct. 2009.

[2] V. Blagojevic and P. Ivanis, "Ergodic capacity for TAS/MRC spectrum sharing cognitive radio," *IEEE Commun. Lett.*, vol. 16, no. 2, pp. 321–323, Mar. 2012.

[3] F. Khan, K. Tourki, M.-S. Alouini, and K. Qaraqe, "Outage and SER performance of spectrum sharing system with TAS/MRC," in *Proc. IEEE ICC*, Budapest, Hungary, Jun. 2013, pp. 381–385.

[4] R. Sarvendranath and N. B. Mehta, "Antenna selection in interference-constrained underlay cognitive radios: SEP-optimal rule and performance benchmarking," *IEEE Trans. Commun.*, vol. 61, no. 2, pp. 496–506, Feb. 2013.

[5] K. Tourki, F. A. Khan, K. A. Qaraqe, H.-C. Yang, and M.-S. Alouini, "Exact performance analysis of MIMO cognitive radio systems using transmit antenna selection," *IEEE J. Sel. Areas Commun.*, vol. 32, no. 3, pp. 425–438, Mar. 2014.

[6] Y. Deng, L. Wang, M. Elkashlan, K. J. Kim, and T. Q. Duong, "Ergodic capacity of cognitive TAS/GSC relaying in Nakagami-m fading channels," in *Proc. IEEE ICC*, Sydney, NSW, Australia, Jun. 2014, pp. 5359–5364.

[7] P. L. Yeoh, M. Elkashlan, T. Q. Duong, N. Yang, and D. B. da Costa, "Transmit antenna selection for interference management in cognitive relay networks," *IEEE Trans. Veh. Technol.*, vol. 63, no. 7, pp. 3250–3262, Sep. 2014.

[8] P. L. Yeoh, M. Elkashlan, T. Q. Duong, N. Yang, and D. B. da Costa, "Transmit antenna selection in cognitive relay networks with Nakagami-m fading," in *Proc. IEEE ICC*, Budapest, Hungary, Jun. 2013, pp. 2775–2779.

[9] P. L. Yeoh, M. Elkashlan, K. J. Kim, T. Q. Duong, and G. K. Karagiannidis, "Cognitive MIMO relaying with multiple primary transceivers," in *Proc. IEEE GLOBECOM*, Atlanta, GA, USA, Dec. 2013, pp. 1956–1961.

[10] T. Wang, A. Cano, G. B. Giannakis, and J. N. Laneman, "High-performance cooperative demodulation with decode-and-forward relays," *IEEE Trans. Commun.*, vol. 55, no. 7, pp. 1427–1438, Jul. 2007.

[11] I. S. Gradshteyn and I. M. Ryzhik, *Table of Integrals, Series and Products*, 6th ed. New York, NY, USA: Academic, 2000.

Vehicle Lateral Dynamics Control Through AFS/DYC and Robust Gain-Scheduling Approach

Hui Zhang and Junmin Wang

***Abstract*—In this paper, we investigate the combined active front-wheel steering/direct yaw-moment control for the improvement of vehicle lateral stability and vehicle handling performance. A more practical assumption in this work is that the longitudinal velocity is not constant but varying within a range. Both the nonlinear tire model and the variation of longitudinal velocity are considered in vehicle system modeling. A linear-parameter-varying model with norm-bounded uncertainties is obtained. To track the system reference, a generalized proportional–integral (PI) control law is proposed. Since it is difficult to get the analytic solution for the PI gains, an augmented system is developed, and the PI control is then converted into the state-feedback control for the augmented system. Both the stability and the energy-to-peak performance of the augmented system are explored. Based on the analysis results, the controller-gain tuning method is proposed. The proposed control law and controller design method are illustrated via an electric vehicle model.**

***Index Terms*—Active front-wheel steering (AFS), direct yaw-moment control (DYC), robust gain-scheduling control.**

I. INTRODUCTION

The last decades have witnessed increasing efforts for the vehicle advanced control systems [1], [2]. Generally, the vehicle advanced control systems are developed to improve fuel economy, emissions, passenger comfort, stability and safety, the driver's feeling, etc. For fuel economy, the technologies include the hybrid electric vehicles and electric vehicles (see [3]–[7] and the references therein). To reduce the emissions, the selective catalytic reduction control systems and EGR systems can be seen in [8], [9] for Diesel engines. Semiactive/active suspension systems with advanced control strategies have been used to improve passenger comfort [10]–[13]. To improve stability and vehicle handling, there are antilock braking systems [14]–[17], active front-wheel steering (AFS) systems [18], direct yaw-moment control (DYC) [19], [20], and some integrated control systems [21], [22]. It is of no doubt that, with the new control technologies emerging and the increasing requirements on vehicle performance, the vehicle advanced control systems will still be popular topics during the near future.

For vehicle stability control, the DYC is one of the most concerned topics. The main principle of DYC is to exert an external yaw moment to control the lateral motion of vehicles during severe driving maneuvers. The main problems of DYC arise from how to calculate the optimal yaw moment and how to generate the desired moment. In [23], Sawase and Sano introduced an active yaw control system that

Manuscript received September 26, 2014; revised December 11, 2014; accepted January 9, 2015. Date of publication January 12, 2015; date of current version January 13, 2016. The work of H. Zhang was supported in part by the National Science Foundation of China under Grant 61403252, by the Program for Professor of Special Appointment (Eastern Scholar) at the Shanghai Institutions of Higher Learning under Grant TP2014053, and by the Innovation Program of Shanghai Municipal Education Commission under Grant 15ZZ077.

H. Zhang is with the Merchant Marine College, Shanghai Maritime University, Shanghai 201306, China (e-mail: huizhang285@gmail.com).

J. Wang is with the Department of Mechanical and Aerospace Engineering, The Ohio State University, Columbus, OH 43210 USA (e-mail: wang.1381@osu.edu).

Color versions of one or more of the figures in this paper are available online at http://ieeexplore.ieee.org.

Digital Object Identifier 10.1109/TVT.2015.2391184